# Chaotic and periodic passive $Q$ switching in coupled $CO_2$ lasers with a saturable absorber

Yudong Liu,* P. C. de Oliveira,† M. B. Danailov,‡ and J. R. Rios Leite
*Departamento de Física, Universidade Federal de Pernambuco, 50739 Recife, Pernambuco Brazil*
(Received 30 November 1993; revised manuscript received 6 April 1994)

Two $CO_2$ lasers with $SF_6$ as an intracavity saturable absorber were optically coupled, and their passive $Q$-switching dynamics were investigated. The amount of coupling used induced transitions from two unsynchronized periodic oscillating lasers into two synchronized chaotic ones. Conversely, the uncoupled lasers set in the chaotic regime could be made synchronized with a periodic pulsation after their coupling. Numerical solutions for the laser equations agree with the observations.

PACS number(s): 42.65.Pc, 42.50.Lc, 42.50.Ne, 42.60.Gd

## I. INTRODUCTION

Dynamical systems in high dimensional manifolds are an open subject of mathematical and physical studies [1,2] and some of their properties may be studied starting from its lower dimensional subsystems [3,4]. In optics, the multimode laser instabilities [5,6] and the transverse nonlinear optics instabilities [7] are among the problems in that large framework.

Here we study experimentally and numerically the dynamics of two single mode $CO_2$ lasers with intracavity saturable absorber when they are submitted to variable amount of optical coupling. When isolated this type of lasers have been extensively studied [8–12]. Under appropriate conditions the saturable absorber leads the continuously operating laser into a periodic passive $Q$-switching instability by a subcritical Hopf bifurcation. Further change in a control parameter produces cascade period doubling and type I intermittence with Shil'nikov homoclinic orbits giving routes to chaos verified experimentally and numerically [8–12]. The numerical results are obtained from a model where the absorber is a two level resonant absorbing medium and the amplifier is described by a three level medium [9]. In the mostly studied cases of $CO_2$ laser with molecular absorber ($SF_6$, $CH_3I$, etc.) the first instability has pulses with frequency in the range of 50 kHz. When one of the parameters like the absorber gas pressure or the cavity tuning is changed this frequency changes and lower frequency features appear, showing a widely studied scenario of chaotic pulsation [8–12].

In our experiments two such lasers were optically coupled by sending part of each output beam into the other laser cavity. As shown below, even for a small amount of coupling (<6%) their dynamics changes with a rich variety of possibilities. For instance, the two lasers may be in stable cw condition but the extra beam intensity due to the coupling creates an effective higher saturation and makes one or both cross the threshold for pulsed $Q$-switching operation. This occurs without any change in the lasers pumping rates. Thus periodic or chaotic pulsations may result from the coupling. Numerically and experimentally we show that if the coupling is mainly on the lasers absorber it induces positive correlated pulsations while for the coupling on the gain media only there will be negative correlation between the pulses of the two lasers. This last effect is analogous to the mode hopping in two mode pulsed lasers (the modes compete for the same gain) [13]. Other behavior observed on the coupled system is not directly intuitive. The two lasers may be in a chaotic uncorrelated regime when isolated and by the coupling both fall in a synchronized periodic regime. Similarly, two lasers may be in uncorrelated periodic oscillations and after coupling both are synchronized periodic or chaotic. All these experimental features were predicted numerically [14] and observed as discussed below.

## II. THE EXPERIMENT

The two lasers used in the experiment are depicted in Fig. 1. Laser $A$ had a 150 cm long cavity with a 5 m radius of curvature gold coated mirror at one end and a 150 gr/mm diffraction grating on the other. The mirror was mounted on a piezoelectric transducer (PZT) ceramic for fine frequency cavity tuning (60 MHz) within each $CO_2$ line. A grating reflecting 70% on first order selected single $CO_2$ emission and gave the output power by means of its 30% zero order reflection. The gain medium was a water cooled 90 cm long Pyrex tube with 1.0 cm diameter, ended by two NaCl Brewster windows. A mixture of $CO_2$, $N_2$, and He, in the proportion of 1:1:4, flew with an average pressure of 10 Torr. A stable high voltage power supply excited the mixture with 15 mA. The intracavity

*Present address: Departamento de Eletrônica Quântica, Universidade Estadual de Campinas, SP Brazil.
†Permanent address: Departamento de Física, Universidade Federal da Paraíba, 58051-970 João Pessoa, PB Brazil. Electronic address: paulo@df.ufpe.br
‡Permanent address: Faculty of Physics, Sofia University, Sofia, Bulgaria.

 

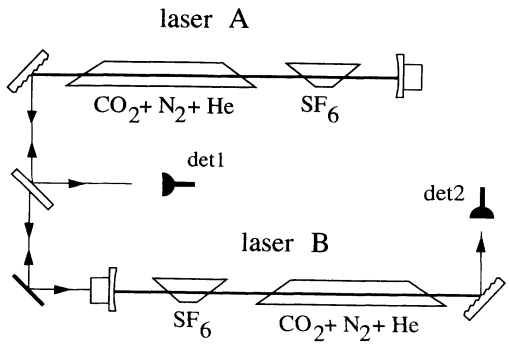


FIG. 1. Scheme of the two coupled $CO_2$ lasers with saturable absorbers. The lasers were 15 m apart and their characteristics are described in the text.

saturable absorber cell also had NaCl Brewster windows and was 5.5 cm long.

Laser $B$ was similar to $A$ but its cavity was 185 cm long. Its diffraction grating only coupled out 1.7% of the in-cavity power and the main output coupling was a germanium 5 m curvature mirror made for 20% transmission at 10 $\mu$m. The gain medium of laser $B$ was 75 cm long ended by ZnSe Brewster windows and the exciting current for the gas mixture was 10 mA. Its saturable absorber cell was also 5.5 cm long.

Lasers $A$ and $B$ were 15 m apart and to achieve their optical coupling two collimating (5 m radius of curvature) mirrors were used. Figure 1 shows how the output from the grating of laser $A$ was coupled to the output mirror of laser $B$. The lasers had parallel linearly polarized output. The power coupling from laser $A$ into laser $B$ (and $B$ into $A$) were measured to be $5.0 \pm 0.5\%$. The two laser outputs were monitored by HgCdTe photodiodes. A spectrum analyzer was used to monitor the optical beatnote of the two lasers during the experiments. Typical relative frequency jitter was 700 kHz and the two lasers, operating in the same line, could be PZT tuned up to $\pm$ 30 MHz. The high frequency jitter observed between the lasers ($\geq$ 500 kHz) allows us to assume that in the time scale of their $Q$ switching ($\geq$ 20 $\mu$s) any interference between the two laser fields is averaged to zero. Without gas in the absorbing cells the lasers were coupled and some changes in their steady operation state was only detected when their detuning was very small ($<$ 1 MHz). Avoiding this condition the dynamical changes studied here were associated to the lasers with the intracavity saturable absorber and different from the case of regular lasers coupled with injected signal [15,16].

With the two laser gratings selecting the 10.6 $\mu$m $P(18)$ $CO_2$ line, the strong resonance coincidence with the $A_2^1P(33)$ line of $SF_6$ leads to passive $Q$ switching instability of the lasers at a wide range of pressures of $SF_6$

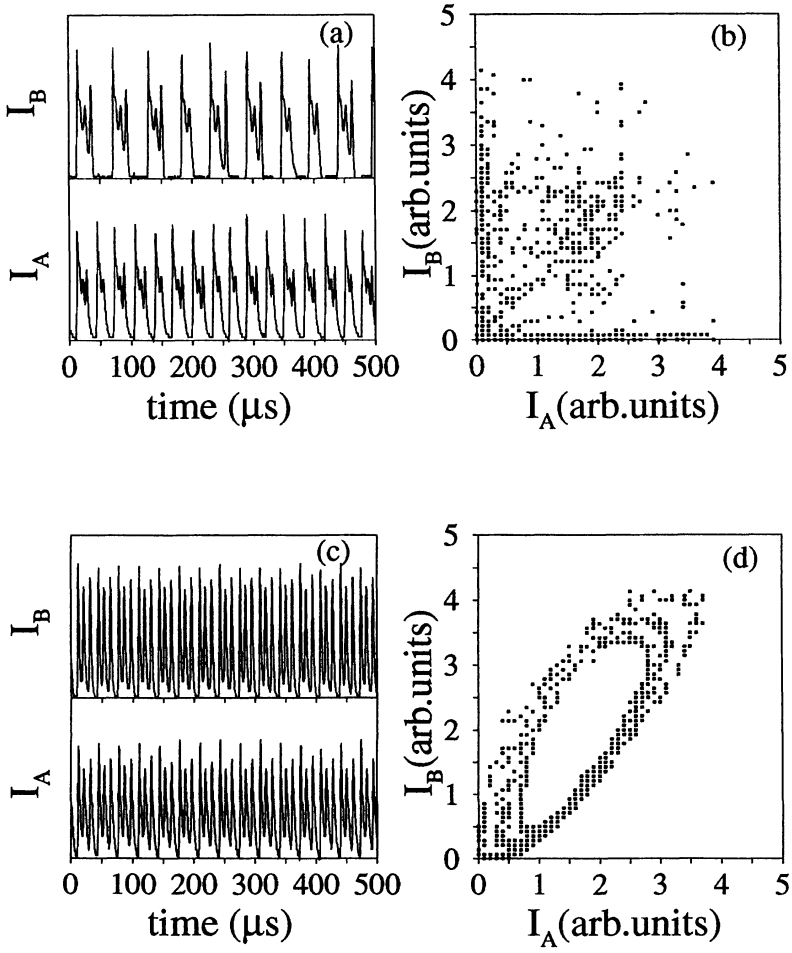


FIG. 2. Passive $Q$ switching of the two $CO_2$ lasers. (a) Before their optical coupling the two lasers are in chaotic pulsations not synchronized. (b) Correlation diagram of the unsynchronized laser intensities. (c) Lasers' pulsations and (d) intensity correlation after optical coupling of the two lasers. The lasers were oscillating at the same optical frequency, with a relative jitter much faster than the observed pulsation rates.

in the intracavity cell. A buffer gas is usually mixed with $SF_6$ to control the ratio of linear absorption to saturation intensity in the dynamics of the saturable absorber. Figure 2 shows the output pulses of the lasers when the intracavity cell of laser $A$ had 40 m Torr of $SF_6$ mixed with 600 m Torr of $CO_2$ as a buffer (in the cell the $CO_2$ is mostly in its vibrational ground state and will not absorb the laser light) while laser $B$ had 20 m Torr of $SF_6$ plus 700 m Torr of $CO_2$ for laser $B$. Choosing the appropriate PZT cavity frequency tuning the uncoupled lasers were set in chaotic pulsation as given in Fig. 2(a). Unblocking the optical path that couples the two lasers gave Fig. 2(c). The lasers synchronized their pulsations and became periodic. Figures 2(b) and 2(d) are the two intensity correlations of Figs. 2(a) and 2(c), respectively. For another PZT tuning, when the two lasers frequencies were 2 MHz apart and both were in periodic regime when isolated [Fig. 3(a)], the coupling led them into synchronized chaotic oscillations as shown in Fig. 3(c).

The collision broadening of the $SF_6$ transition by the $CO_2$ buffer is 10 MHz/Torr while the Doppler linewidth is 30 MHz. Thus, the absorbers were inhomogenously broadened for $P_{CO_2} < 1$ Torr and when the two lasers had optical frequencies differing by more than 10 MHz there was no absorber coupling because each laser saturated a different axial velocity. Both lasers had lower saturation intensities in their absorbers as compared to their amplifiers and so their coupling acted mostly as absorber coupling when the lasers had their optical frequencies separated by less than 5 MHz. Positive correlation between their pulsation resulted as shown in Figs. 2(d) and 3(d). The case of anticorrelated synchronization was obtained when the optical frequency detuning of the lasers was 20 MHz. Before coupling they were periodic, in $P^{(0)}$ and $P^{(1)}$ regimes [11], respectively, as shown in Fig. 4. After coupling each laser kept the same type of periodic pulse shape but they adjusted their pulse rate and separation to meet the negative correlation condition. Another experimental coupling was obtained using cross linear polarized lasers. Then all field interferences were further eliminated at the expenses of smaller coupling coefficient due to the Brewster windows in the lasers. Again the coupling between absorbers induced positive correlated synchronization of the periodic pulsations very similar to the ones shown in Figs. 2 and 3. When the detuning of the lasers was bigger than the absorbers homogeneous linewidths we also observed the anticorrelated pulsations.

Summarizing the experimental observations for the coupling instabilities, three regions of frequency detuning can be described: (a) for less than 5 MHz detuning between the lasers the coupling of power from a laser on the absorber of the other could be dominant and synchronized periodic and chaotic pulsation could be induced; (b) intermediate detuning 5 MHz $< \Delta\nu <$ 10 MHz al-

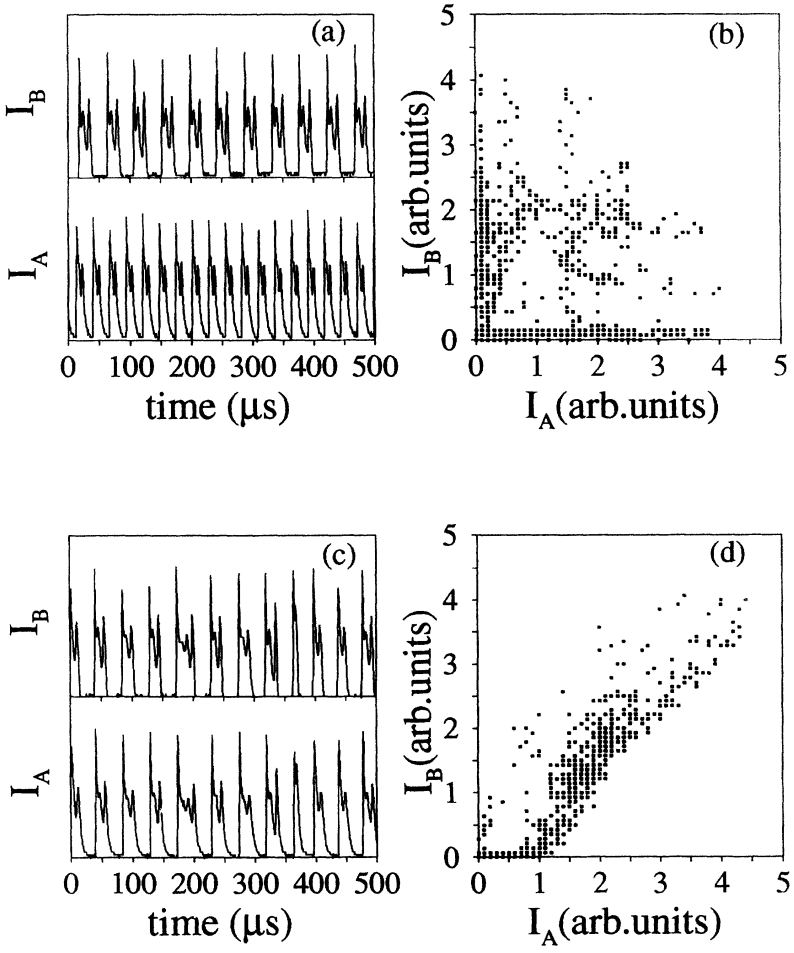


FIG. 3. Passive $Q$ switching of the $CO_2$ lasers. (a) Before coupling the two lasers are periodically pulsing but unsynchronized. (b) Intensities' correlation of uncoupled lasers. After coupling (c) the lasers became synchronized chaotic and their intensities show (d) a positive degree of correlation. Laser detuning was 2 MHz.

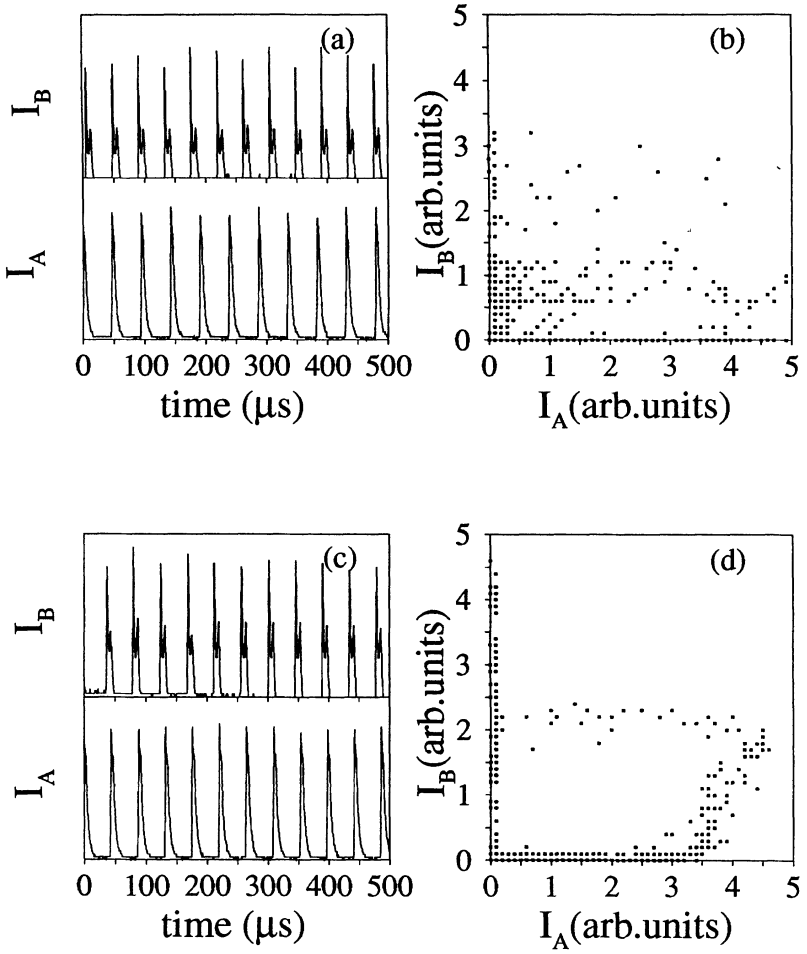


FIG. 4. Passive $Q$ switching of the $CO_2$ lasers. (a) Before coupling the two lasers are periodically pulsing but unsynchronized. (b) The intensities' correlation is null. After coupling (c) the lasers remain periodic but became synchronized in anticoincidence pulsation. Their intensities show (d) a negative degree of correlation. The coupling was on the amplifiers and the lasers' detuning was 20 MHz.

lowed coupling in both absorber and amplifier showing chaotic instabilities without synchronization; (c) with large detuning, $\Delta\nu \sim 20$ MHz the dominant coupling was on the amplifiers and antisynchronized pulsations resulted.

## III. THE MODEL AND THE NUMERICAL SOLUTIONS

The theoretical model used to describe the laser with a saturable absorber by the two level-three level systems of rate equations was introduced by Tachikawa *et al.* [9]. Following the approximations and notation used in Refs. [11,14] laser $A$ is described by

$$\dot{I}_A = I_A(U_A - \overline{U}_A - 1) , \quad (1)$$

$$\dot{U}_A = \epsilon_A \left[W_A - U_A(1 + I_A + C_1 I_B)\right] , \quad (2)$$

$$\dot{W}_A = \epsilon_A \left[A_A + b_A U_A - W_A\right] , \quad (3)$$

$$\dot{\overline{U}}_A = \bar{\epsilon}_A \left\{\overline{A}_A - \overline{U}_A[1 + a_A(I_A + C_2 I_B)]\right\} . \quad (4)$$

Similar equations hold for laser $B$. In these equations $I_A$ is the inside cavity average intensity, $U_A$ is the normalized gain medium population difference, $W_A$ represents an effective population describing the three level population conservation of the gain medium and $\overline{U}_A$ is the normalized population difference of the two level absorber. The time unit is the laser cavity lifetime [thus the $-1$ in Eq. (1)]. The other parameters in the equations are $\epsilon_A$ the normalized relaxation rate for the gain medium population difference, $C_1$ the amplifier coupling coefficient (assumed symmetrical) between laser $A$ and $B$; $A_A/(1 - b_A)$ the gain population inversion and $\overline{A}_A$ is the absorber population inversion at no laser oscillation, $b_A$ the ratio between relaxation rates of the two gain medium levels, $\bar{\epsilon}_A$ is the normalized relaxation rate of the absorber; $a_A$ the ratio between the saturation intensities of the absorber and the gain media transitions and $C_2$ the coupling coefficient of the two lasers absorbers. Detailed explanation of these dimensionless quantities and the physical behavior contained in Eqs. (1)–(4) are given in Ref. [11].

The numerical solutions of Eqs. (1)–(4) along with the corresponding four equations for laser $B$ give rise to $Q$-switching pulsations with all characteristics observed experimentally as shown in Figs. 2–4. The choice of parameters for each laser was made as in Refs. [11,14], to produce pulsed solutions as previously observed in experiments. The coupling coefficients were assumed in the range of less than 6%, according to our experimental val-

ues. The high laser frequency detuning was simulated by taking $C_1 = 0$, i.e., no cross saturation or coupling in the absorbers. Figure 5 shows the numerical results when we set the parameters of the uncoupled lasers to reproduce the so called $C^{(2)}$ chaotic pulsation which occurs between $P^{(2)}$ and $P^{(3)}$ periodic regimes as noted in Ref. [11]. The pulses shown in Fig. 5(a) should be compared with the experimental results of Fig. 2(a). The $I_A$ versus $I_B$ plot is given in Fig. 5(b) which should be compared with the experimental results of Fig. 2(b), where low pulse correlation appear. Solutions with the same parameters and including coupling coefficients $C_1 = C_2 = 5\%$ are shown in Fig. 5(c). Now the solutions for both lasers became periodic $P^{(2)}$, the lasers synchronize and acquired positive correlation [Fig. 5(d)] in their pulses. This is to be compared with the experimental observation of Figs. 2(c) and 2(d), where the same type of pulses and synchronization was obtained with a higher degree of positive correlation. Here we should note that the spikes of the experimental pulses were shorter than the numerical ones due to limited time constant in detection. This explains partially the differences between Figs. 2(d) and 5(d).

Bifurcation diagrams for the different dynamical states of the coupled lasers were numerically obtained by varying the coupling coefficients in the lasers equations. Figures 8 and 9 show an example of dynamical bifurcations when the lasers are weakly coupled by their amplifiers, with $C_1 = 0.05$ and the coupling coefficient for the absorbers is increased. The parameters in the equations were chosen to have both lasers chaotically pulsing when isolated. The small amplifiers coupling, without absorber coupling, produces the already mentioned antisynchronization between the two laser pulses as shown in Fig. 6(a). As $C_2$ increases, i.e., as the coupling between absorbers is introduced, a competition between positive and negative synchronization sets in. Simultaneously the dynamics of the two lasers evolves through chaotic and periodic bifurcations. Figure 6(b) shows how the two laser intensities became chaotic when $C_2 = 0.01$. Further, increasing the absorber coupling show the recovery of periodic pulsation for the two lasers. What was verified (unfortunately extensive search for different parameters in the equations were not done to allow general statements) was a cascade of period doubling leading the lasers from the chaos, shown in Fig. 6(b), into positively correlated periodic pulsation, as seen in Fig. 6(c). Increasing the absorber coupling coefficient beyond 4.2% reestablishes the chaotic pulsations, but now with a positive degree of correlation, that can be observed in Fig. 6(d). This may be explained by arguing that the amplifier coupling dominates for the purpose of synchronization, despite the fact that chaotic dynamics is on. Figure 7 shows the corresponding $I_A$ versus $I_B$ phase diagrams associated to the time series shown in Figs. 6(a)–

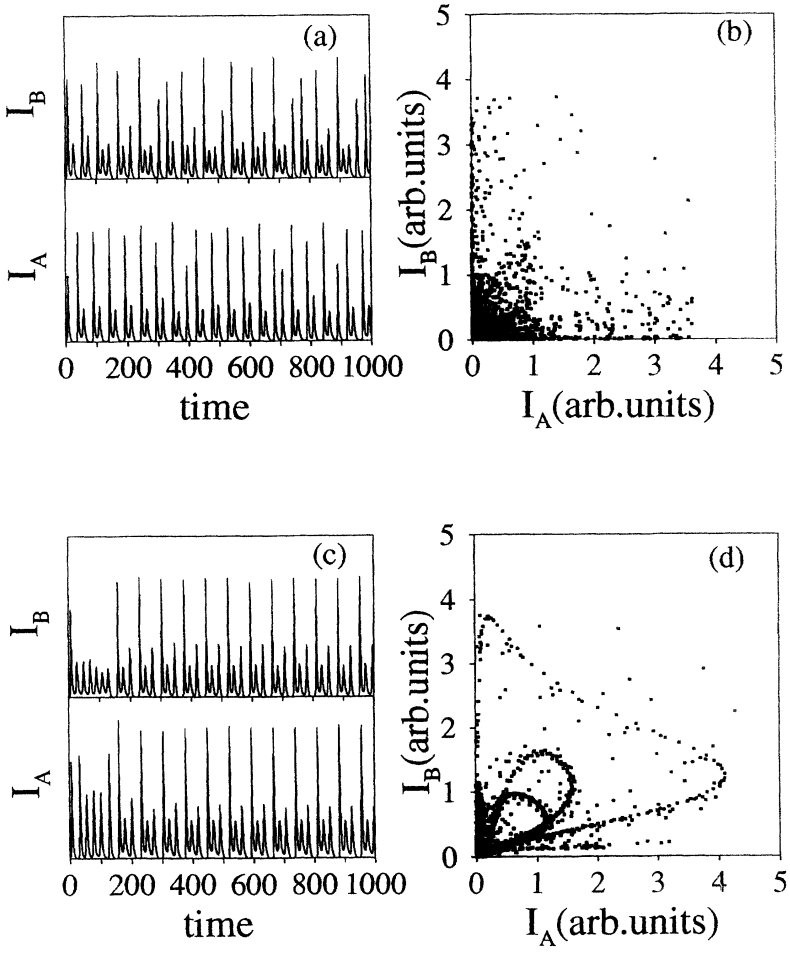


FIG. 5. Numerical solutions of coupled laser system equations. Laser $A$: $\epsilon = 0.137$, $\bar{\epsilon} = 1.6$, $A = 1.701\,39$, $\bar{A} = 1.960\,35$, $a = 4.17$, $b = 0.85$. Laser $B$: $\epsilon = 0.137$, $\bar{\epsilon} = 4.6$, $A = 1.795\,79$, $\bar{A} = 1.985\,10$, $a = 4.17$, $b = 0.85$. (a) Before coupling each laser is chaotic and (b) their intensities are uncorrelated. (c) Pulses after coupling with $C_1 = C_2 = 5\%$ and (d) their intensities' correlation.

6(d). The figures showing lower density of points along the diagonal describe the negatively correlated signals, as in Figs. 6(a) and 6(b), while higher density along the diagonal mean positively correlated (synchronized) pulses, as in Figs. 6(c) and 6(d). The full bifurcation diagram described above is given in Fig. 8, where the maxima of the intensity of laser $A$ are represented, for $C_2$ between 0 and 5%. Regions of periodic pulsation correspond to a finite number of values for the maxima as in $a$ and $c$ in the figure. The shaded areas marked as $b$ and $d$ are the chaotic domains. The lasers synchronization was inspected directly on the pulses intensity diagram and through a numerical algorithm to calculate the degree of correlation between two data time sequences. A two signal correlation can be defined as

$$C(\tau) = \frac{\sum_{i=1}^{N} (x_i - \overline{x})(y_{i+\tau} - \overline{y})}{\left[\sum_{i=1}^{N} (x_i - \overline{x})^2 \sum_{i=1}^{N} (y_{i+\tau} - \overline{y})^2\right]^{1/2}}, \quad (5)$$

where $x_i$ and $y_i$ represent time sequences of dynamical variables with $\overline{x}$ and $\overline{y}$ the respective averages. $N$ is the number of points of the time sequences and $\tau$ is the time

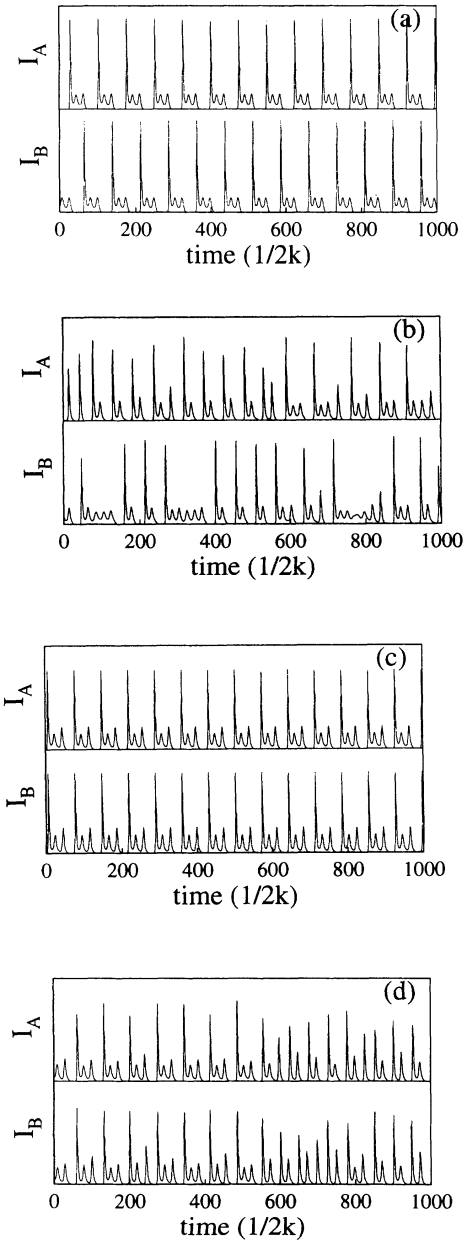


FIG. 6. Numerical solutions of coupled laser system equations for some values of the absorbers coupling coefficient $C_2$, with a fixed value of 5% for the gains coupling coefficient $C_1$. (a) $C_2 = 0.00$; (b) $C_2 = 0.01$; (c) $C_2 = 0.03$; (d) $C_2 = 0.048$. Laser $A$: $\epsilon = 0.1369$, $\overline{\epsilon} = 1.182$, $A = 1.845$, $\overline{A} = 2.16$, $a = 4.17$, $b = 0.847$. Laser $B$: the same parameters, except $A = 1.863$.

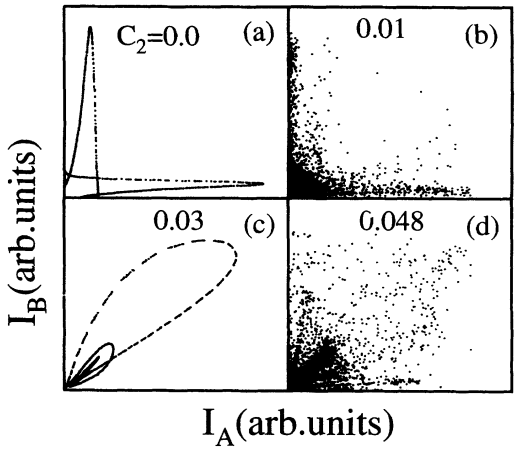


FIG. 7. Numerical solutions of the coupled laser system of equations calculated with the same parameters as Fig. 6. Pulse intensities' correlations show evolution from (a) antisynchronized periodic pulses to (b) partially antisynchronized chaos then back to (c) periodic but positively synchronized periodic and finally (d) into chaos maintaining synchronization.

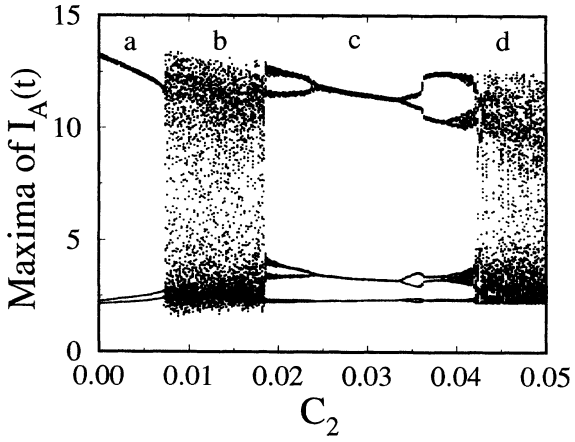


FIG. 8. Bifurcation diagram of the coupled lasers dynamics as calculated on the maxima of one laser intensity, as a function of the coupling coefficient of the absorbers. Region (a) corresponds to periodic pulses with negative correlation; (b) shows chaos with partial negative correlation; (c) has the period doubling cascade back into periodic pulsation but with positive correlation; and finally (d) chaos is reestablished now with positive correlation. The parameters used were the ones of Figs. 6 and 7.

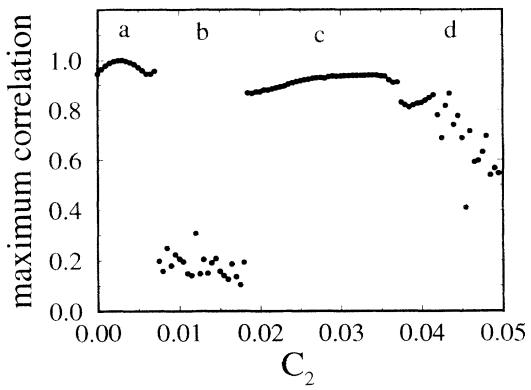


FIG. 9. Bifurcation diagram of the coupled laser dynamics as manifested on the absolute value of the maximum of the correlation function of the two laser intensities, calculated as a function of the coupling coefficient of the absorbers. Region (a) corresponds to periodic pulses with negative correlation; (b) shows chaos with small (negative) correlation; (c) has the period doubling cascade back into periodic pulsation but with positive correlation; and finally (d) chaos is reestablished now with positive correlation. The parameters used were the ones of Figs. 6, 7, and 8.

delay introduced between the sequences, in units of the sampling interval. One expects $C(\tau) = 0$, independent of $\tau$, for two totally uncorrelated sequences and $C(0) = 1$ for perfectly synchronized signals. When the signals have a certain degree of correlation $C(\tau) \neq 0$. Negative values meaning an antisynchronization. The best manner to find the degree of correlation is to find the maximum of $C(\tau)$. If it occurs for $\tau = 0$ the correlation is positive and if it occurs for a non-null value of $\tau$ close to half the period, or half the quasiperiods in the case of chaotic signals, the two signals are antisynchronized.

The maximum of the correlation of the two laser intensities using Eq. (5) with the numerical data series of the bifurcation diagram of Fig. 8 is given in Fig. 9. As it can be seen in Fig. 9 region *a* shows maximum correlation. However, it does occur for a delay of half the quasiperiod of the pulsation and so it corresponds to an antisynchronized periodic pulsations regime, consistent with Fig. 6(a). The region *b* shows a small amount of (negative) correlation and therefore describes a partially synchronized chaotic pulsations. The segment *c* corresponds to maximum correlation at no delay which is the signature of synchronized periodic pulsations and *d* has a decreasing correlation also at no delay as function of the absorber coupling, indicating partially synchronized chaotic pulsations. Further studies of the properties of the coupled lasers bifurcation dynamics is under investigation; the above correlation function being used systematically throughout the bifurcation diagrams for many sets of equations parameters.

## IV. CONCLUSIONS

Considering our crude model neglecting standing wave effects, inhomogeneous broadening in the absorber medium, transverse beam profile effects and other approximations, there is a very good agreement between the calculations with a rate equations and our experiments for the coupling of two lasers with saturable absorber. The numerical results contain the essential features of the experiments shown in Figs. 2 to 4 and we conclude that the main properties of the dynamics of coupled $CO_2$ lasers with saturable absorber might be understood by a system of coupled rate equations. Further properties of this system await a detailed study and in particular the phenomena of partial synchronization demonstrated here will be inspected from the point of view of the templates for the chaotic attractors of the laser with saturable absorber [12].

*Note added in proof.* Sugawara *et al.* [Phys. Rev. Lett. **72**, 3502 (1994)], demonstrated two $CO_2$ lasers' synchronization in a master-slave configuration.

## ACKNOWLEDGMENTS

The authors acknowledge support from Conselho Nacional de Desenvolvimento Científico e Tecnológico (CNPq) and Fundação de Ciências de Pernambuco (FACEPE), Brazil.

[1] L. M. Pecora and T. L. Carroll, Phys. Rev. Lett. **64,** 821 (1990).
[2] J. M. Kowalski, G. L. Albert, and G.W. Gross, Phys. Rev. A **42,** 6260 (1990).
[3] F. Mossayebi, H. K. Qammar, and T. T. Hartley, Phys. Lett. **161,** 255 (1991).
[4] L. M. Pecora and T. L. Carroll, Phys. Rev. Lett. **67,** 945 (1991).
[5] L. M. Narducci and N. B. Abraham, *Laser Instabilities and Laser Physics* (World Scientific, Singapore, 1988).
[6] D. Hennequin, D. Dangoisse, and P. Glorieux, Opt. Commun. **79,** 200 (1990).
[7] A. Blouin, A. Maitre, M. Pinard, J. R. Rios Leite, R. W. Boyd, J. Y. Courtois, and G. Grynberg, Nonlinear Opt. **5,** 469 (1992).
[8] K. Tanii, M. Tachikawa, T. Tohei, F. L. Hong, and T. Shimizu, Phys. Rev. A **43,** 1498 (1991).
[9] M. Tachikawa, F. L. Hong, K. Tanii, and T. Shimizu, Phys. Rev. Lett. **60,** 2266 (1988).
[10] F. de Tomasi, D. Hennequin, B. Zambon, and E. Arimondo, J. Opt. Soc. Am. B **6,** 45 (1989).
[11] M. Lefranc, D. Hennequin, and D. Dangoisse, J. Opt. Soc. Am. B **8,** 239 (1991).
[12] F. Papoff, A. Fioretti, E. Arimondo, G. B. Mindlin, H. Solari, and R. Gilmori, Phys. Rev. Lett. **68,** 1128 (1992).
[13] K. Otsuka, Phys. Rev. Lett. **67,** 1090 (1991).
[14] Y. Liu and J. R. Rios Leite, Phys. Lett. A (to be published).
[15] J. R. Tredicce, F. T. Arecchi, G. L. Lippi, and G. P. Puccioni, J. Opt. Soc. Am. B **2,** 173 (1985).
[16] J. L. Boulnois, A. Vanlerberghe, P. Cottin, F. T. Arecchi, and G. P. Puccioni, Opt. Commun. **58,** 124 (1986).